Next-Gen Manipulation: An Active Surface-Based Underactuated Gripper with Visual Feedback

Karthik Swaminathan*, Mohammed Saad Hashmi*, Alqama Shaikh, Vikas Phalle

***Abstract*—End-effectors in a robotic system generally have the role of executing operations related to manipulating and handling the objects. The traditional grippers are restricted to the scope of performing a specific task, which limits their capability of adapting to changes in the physical properties of the objects. The grippers can become more efficient when integrated with a sub-system catering to manipulating varied-sized objects within the existing gripper workspace. Many state-of-the-art methods have used tendon-based and active surface (belt-driven) actuation techniques to effectively change the pose of a wide range of objects within the gripper (in hand). We propose the design of a gripper system that leverages the role of an active surface-based actuation technique integrated with an underactuated linkage mechanism capable of performing complex manipulations. We have curated an object list, all having different shapes, and executed experimental rotation and translation of objects. We take the help of vision-based feedback to accurately execute targeted goal pose motion and additionally demonstrate the gripper's response to mechanical stresses (through analysis) and grasping an object through torque feedback.**

***Index Terms*— In-hand manipulation, Active-surfaces, Underactuated mechanisms, Bang-Bang controller**

I. Introduction

Grippers have been developed over the years to improve dexterity, reduce the cost of manufacturing, and make simple mechanisms such that desired tasks can be performed. Initial grippers had a very simple design consisting of just two grasping links that could grasp an object but lacked dexterity. To improve the same, the approach presented by [1] introduces the concept of active surfaces, which improves object handling capabilities drastically. For two fingers in an underactuated mechanism with active surfaces [2, 3], the workspace is limited to 2D which gives a maximum of 2 DOF to the object of interest. These surfaces are the subsystems controlled with separate actuators, they add additional degrees of freedom for manipulation. Some approaches [4, 5, 6] involved three grasping links that can also change their configuration in between the manipulation tasks, but this comes at the cost of complex mechanical design and requirement of very specific manufacturing capabilities, which in turn increase the cost of the gripper. Table I shows the comparison between the other two-fingered grippers. There are two aspects of any in-hand object handling task, grasping the object firmly and changing its pose of the object (By rotating or translating the object in different directions). For this, we need some feedback-based mechanism that leverages multiple sensors like magnetic encoders, accelerometers, and MEMS tactile arrays, achieving robust object control. While these sensors enrich feedback [7], they introduce complexity. Notably, direct contact can introduce slight deviations from actual values. To address this in large-scale applications, alternative approaches without on-board sensors are being explored [8]. Using a combination of in-direct torque feedback from the actuator and external visual feedback helps reduce complexity.[9] shows how just visual feedback can help us control the pose of the object. This helps us achieve rotation and translation in the plane of the gripper's workspace. This means there is a necessity for a cost-effective, simple-to-manufacture, and simple-to-control gripper.

Our work is divided into three sections, design, working, and experimentation. We describe the design of the gripper in the gripper description section. We explain the working of the gripper along with the contribution of each component used, and how is the target pose achieved using visual feedback and load feedback from the actuator. Finally, in the experimentation section, we evaluate the gripper's performance over a variety of objects with a given target pose.

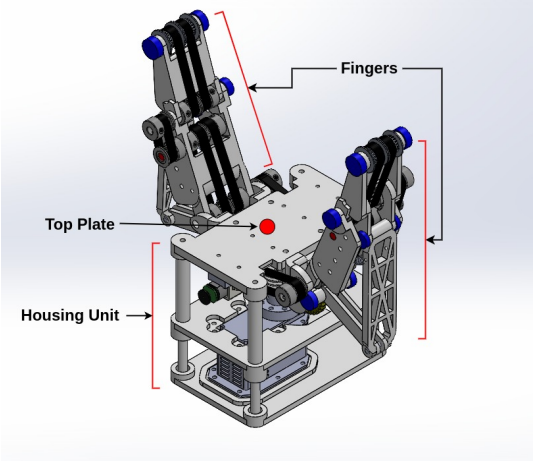

Fig. 1: Isometric view of the gripper showcasing the fingers, motor housing, and active belt system.

II. Gripper Description

A. Design of the Gripper

The design of the gripper consists of two finger units and a housing unit for finger and motor mounts, as illustrated in Fig. 1. The finger primarily consists of 3 submodules, each adding a different functionality to the system. An underactuated Linkage Mechanism is considered to be the skeleton of the finger on which a belt-driven subsystem is integrated

*Denotes Equal Contribution
Department of Mechanical Engineering, VJTI, India

that directly comes in contact with the object when grasped. The whole system is designed using SolidWorks.We used 3D printing for rapid, affordable prototyping, choosing PLA for linkages, gears, and actuator housing. Steel dowel pins served as joints and belt system mounts. The detailed overview of the submodules is mentioned as follows:

1) Linkage Mechanism: Object gripping is powered by the 5 linkage system, where all the links are illustrated in Fig. 2 (a). The linkage mechanism is inspired by an open-source gripper by ALARIS NU [10]. Motion is initiated by the gear system through the transmission link. Under-actuation is made possible by a spring that joins the contact link and connecting link. The spring restricts the relative motion between the contact link and the grasping link. Torque applied to the transmission link causes the connecting link to rise or drop; which turns the grasping link along with the contact link in the inward or outward direction, respectively. In a case where the motion of the contact link is obstructed by the object being grasped, the grasping link is rotated by the connecting link provided the force exerted by the transmission link exceeds the compressive force of the spring.

2) Gear Transmission System: Motion from the motor is effectively transferred to the links via a gear system Fig. 2 (b). It consists of 1 driving worm gear, two intermediate spur gears (module = 1mm) with 30 teeth each, and two driven spur gears (module = 1mm) with 13 teeth each. The worm gear is connected to the MX64 servo to drive the system. Precise finger movement for object handling is ensured by this motion transmission, which starts at the worm gear and is transmitted to the 30-teeth spur gear with a gear ratio of 30:1, which in turn transmits the motion to the 13-teeth spur gear, resulting in a net ratio of 13:1.

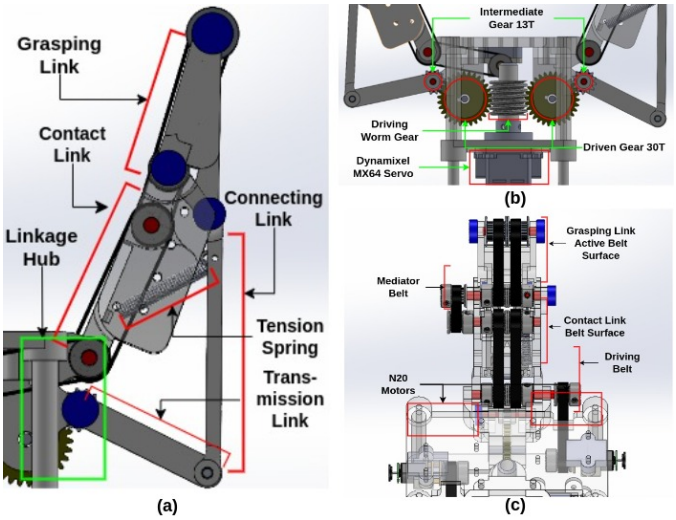

Fig. 2: Gripper Diagrams: (a) Linkage System consisting of four movable links controlled by an underactuated gear system (b) Gear System consisting of connection between worm and spur gears with an effective gear ratio of 13:1 arranged in a planar configuration (c) Belt System highlighting the belt connection between the links

3) Belt Transmission System: Each finger incorporates a belt-drive mechanism with 3 belts. The first belt, driven by the N20 micro gear motor, uses a GT2 timing belt and two 16-teeth pulleys to transmit the motion to the contact link. The second belt runs through the contact link, transferring motion to the grasping link belt via a mediator belt, as shown in Fig. 2(c). This system provides two active belt surfaces per finger, facilitating the increase of active surface area in contact with the object.

III. Working of Gripper

The overview of the setup is shown in Fig. 3, which includes a web camera, gripper, aruco marker, an object of interest, a local PC to run Python scripts, the CM510 controller with U2D2 module, an SRA Board, which contains ESP32-WROOM-32-D as its main MCU.

The Grasping Module is a software component implemented as a Python script. It is designed to continuously monitor and acquire load readings from an MX64 servo motor. The acquired readings are in the range of $0-1023$ and $1024-2047$ for CCW and CW rotation of the shaft of the servo motor, respectively, where 1023 and 2047 depict the maximum achievable torque by the servo motor. The module continuously compares these readings against a predefined threshold, which in this case is set to 125 units, equivalent to 0.733 Nm of torque.

The communication between the local personal computer (PC) and the Dynamixel MX64 motors is facilitated by two intermediary hardware modules: the CM510 and the U2D2. This communication protocol adheres to the half-duplex Universal Asynchronous Receiver Transmitter (UART) standard. In this scheme, the local PC transmits packets containing speed data commands to the motor and subsequently receives packets containing the current load data from the motor in response.

The camera module functions as a visual sensor, providing crucial feedback to the system. Specifically, it detects an Aruco marker affixed to the object of interest. This marker serves as a reference point for the task of pose estimation. The camera continuously captures frames, representing the current pose of the object. Meanwhile, the user defines the desired pose on the local PC, which has an orientation control block running as a Python script on it. This plays a central role in pose control. It calculates the deviation of the current from the desired pose, encompassing both position and orientation. Based on this error, a bang-bang controller is employed to regulate the system's behavior. The pose controller further produces motor commands to manipulate the object and attain the goal orientation or position

Motor control commands originate from the local PC. These commands are transmitted through a web socket connection to the ESP32-WROOM-32D microcontroller, i.e. the main MCU on the SRA-board. The SRA-board, a custom Printed Circuit Board (PCB), serves as the intermediary between the local PC and motor actuation. It receives a 12V power supply and utilizes an LM2576 Buck converter to step down the voltage to 5V, specifically powering the ESP32 microcontroller. Notably, the 12V supply is connected to the TB6612FNG motor driver which drives the N20 motor at a given PWM. The SRA-board receives motor control commands from the local PC through the web socket. A FreeRTOS task running on ESP32 translates

TABLE I: Comparison of various grippers based on Fingers, DoFs, Weight, and Functionalities with our gripper

Grippers	No. of Fingers	DOFs	Underactuation	Active Surface	Weight(in kgs)	Actions Performed
JamHand[11]	2	2	✗	✗	-	Precision Grasp, Power Grasp, Rolling, Translating
D-PALI[12]	2	2	✗	✗	0.1	Pinch Grasp, Rolling, Translating
Model VF[13]	2	2	✗	✗	0.6	Pinch Grasp, Power Grasp, Rolling, Translating
Our Gripper	2	1	✓	✓	0.54	Pinch Grasp, Power Grasp, Rolling, Translating

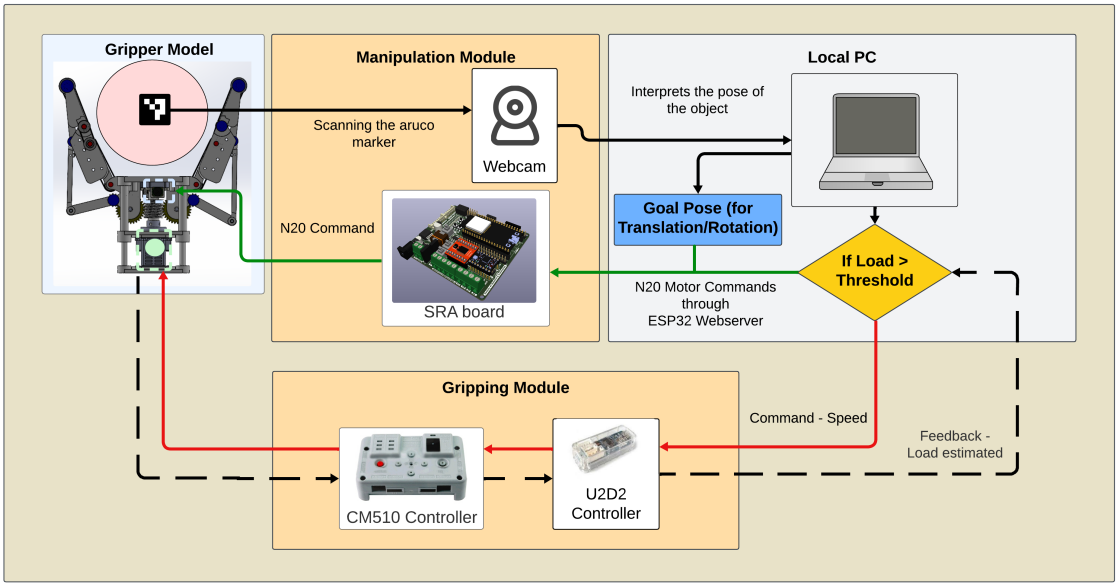

Fig. 3: Process flow diagram: Local PC block acts as a central node where the execution for grasping and manipulation operations are monitored, Gripping module uses CM510 controller with U2D2 communication converter in order to transmit and receive data for Servo motor control, Manipulation module is responsible for controlling the belt motion by deciphering the information fed in the aruco markers attached on the object.

these commands into appropriate Pulse Width Modulation (PWM) signals, a format readily interpretable by the motor driver. These PWM signals are subsequently transmitted to the motor driver, governing the actuation and control of the N20 motor. Thus, the final desired pose of the object is achieved.

IV. Results and Description

A. Analysis and Calculations

1) Structural Analysis: Different sections were analyzed in the system using the ANSYS Student version out of which specific attention was given to the meshing between the gears, as this is a critical area due to the 3D-printed nature of the gears. The possibility of failure was identified in 3 areas: (1) The meshing between the worm and 30T spur gear Fig. 4 (b) where the stress concentration is mainly on the teeth, where the peak stress calculated was 25 MPa at an applied torque of 0.5 Nm; (2) The meshing between 30T and 13T spur gears Fig. 4 (a) where the peak stress attained was 24.6 MPa at an applied torque of 0.5 Nm; and (3) The joint of the contact link and the linkage hub Fig. 4 (c) where the peak stress was 22.9 MPa with a linear vertical force of 50 N, Fig. 4 (d) where the peak stress is mainly on the joint interface of the contact link at 22.9 MPa and the interface of the top plate and linkage hub in the case of the gear housing which is 9.9 MPa. The Yield strength of PLA is approximately 26.91 MPa hence all the above areas are safe.

B. Experimental Setup

While the manipulation capabilities of the gripper are dependent on the type of object and the physical characteristics of the object, we showcase a few examples of In-hand object manipulation as shown in Fig. 5. We consider Cylindrical (Mug), Hexagonal (Pen Stand), Spherical (Ball) and Cuboidal (Box) shapes of objects as our test materials as mentioned in Table II.

TABLE II: Description of objects used for the experiments

Object	Dimensions (in mm)	Type	Weight (in g)	Goal Position (in degrees/in cm)
Mug	105x105x130	Cylindrical	55	30 ± 1.45
Penstand	60x60x80	Hexagonal	110	$2cm \pm 0.75$
Ball	160x160x160	Spherical	115	20 ± 2.5
Box	125x110x60	Cuboidal	175	$1.5cm \pm 0.15$

The two key criteria of any belt-driven system performing manipulation of an object in place are: (1) Making sure the object is within the workspace of the gripper and the object is grasped when the gripper is closed, (2) The traction created between the gripper and the belt should be such that the slippage of the object doesn't take place when grasped. To tackle the first aspect, the objects are placed on the gripper and the finger is rotated with a constant angular speed of 3.3 RPM. The gripper is made to power grasp the object and the underactuated system of the finger ensures the closure of the fingers for grasping. To get an approximate estimate

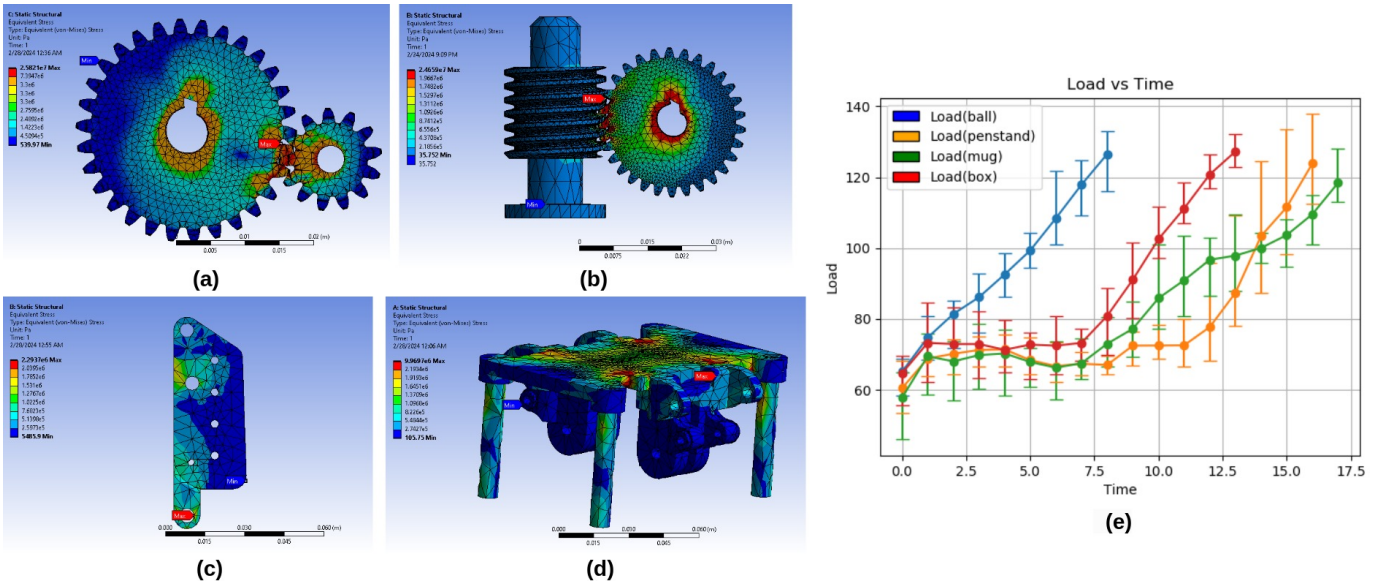

Fig. 4: Stress distribution (a) Spur (30T) with Spur (13T), (b) Spur (30T) with Worm gear, (c) contact link joint, (d) Linkage Hub, (e) Estimation in the variation of load experienced by the Dynamixel motor with time when grasping objects

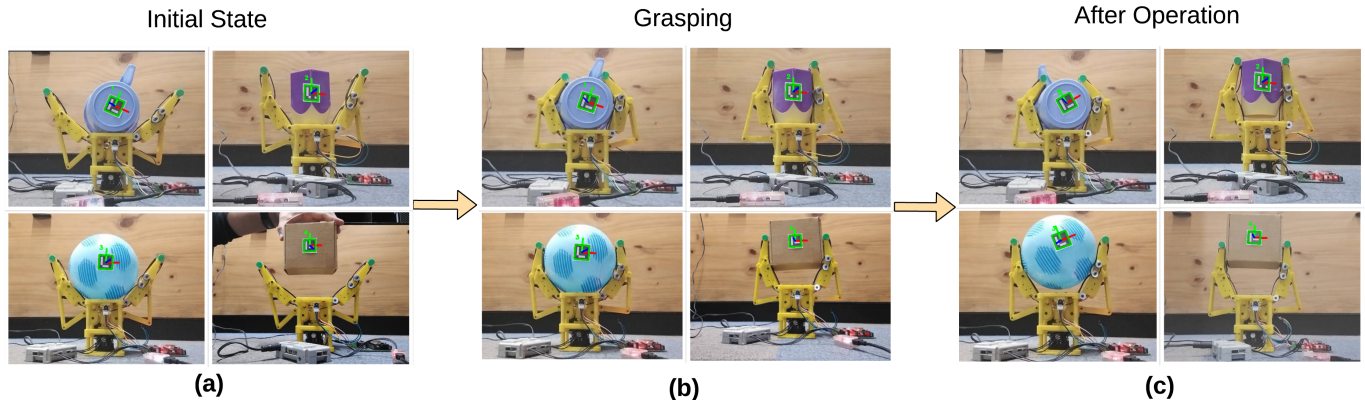

Fig. 5: (a) The initial state of the gripper with four different types of objects placed on it, (b) The gripper grasps the objects, (c) The gripper performs the operation of translation (for the Pen stand and Box) and rotation(for Mug and Ball)

of grasping, the torque feedback from the inbuilt feedback mechanism of the Dynamixel MX64 Motor was utilized and no external torque sensor was used for measurement. The threshold for the load at the level of the gripper is kept in the range of 0.7 to 0.75 Nm accounting for the structure's strength capacity. This ensures the gripper tightly holds the object. Once the object is grasped, visual feedback about "Object's type" and "Object's Pose" is accessed with the use of attached aruco markers. The goal position is provided to the system present within the workspace of the gripper. Using the ESP32 Wifi stack the N20 motor commands are sent to ESP32 keeping the PWM signal value at 50%.

C. Experimental Result

The objects are made to be grasped for 10 iterations from the gripper's home configuration and Fig. 4 (e) highlights the variation in the load values over time. The Y-axis of the plot stating the Load Values are the dynamixel feedback-based load values mentioned in section 3. The plot shows that the trend for the ball is steeper than the other objects as the ball comes in contact much earlier due to its size and achieves a higher load value much earlier. Table II illustrates the properties of the objects used for the experiments. The error column of the table showcases the range of error when the objects i.e. Mug and Ball are rotated to a goal pose (for rotation) of 30 °and 20 °respectively while Pen stand and Box are translated to a goal pose (for translation) of 2cm and 1.5cm respectively.

V. Conclusion

Through the research and analysis, we present the active surface, simple to manufacture, and control design of a gripper. This gripper has a mechanically intelligent 5-bar linkage mechanism, which allows both fingers to be controlled by a single actuator. We demonstrated pose control over 4 objects of different shapes and structural strength at the critical failure points, demonstrating the adaptability and robustness of the proposed gripper. In future work, we would extend the research to bring in modularity (in the design space) to cater to any shape and property of the object.

References

[1] V. Tincani, M. Catalano, E. Farnioli, M. Garabini, G. Grioli, G. Fantoni, and A. Bicchi, "Velvet fingers: A dexterous gripper with active surfaces," *Proceedings of the ... IEEE/RSJ International Conference on Intelligent Robots and Systems. IEEE/RSJ International Conference on Intelligent Robots and Systems*, pp. 1257–1263, 10 2012.

[2] *In-Hand Manipulation Primitives for a Minimal, Underactuated Gripper With Active Surfaces*, ser. International Design Engineering Technical Conferences and Computers and Information in Engineering Conference, vol. Volume 5A: 40th Mechanisms and Robotics Conference, 08 2016. [Online]. Available: https://doi.org/10.1115/DETC2016-60354

[3] A. Kakogawa, H. Nishimura, and S. Ma, "Underactuated modular finger with pull-in mechanism for a robotic gripper," in *2016 IEEE International Conference on Robotics and Biomimetics (ROBIO)*, 2016, pp. 556–561.

[4] Y.-J. Kim, H. Song, and C.-Y. Maeng, "Blt gripper: An adaptive gripper with active transition capability between precise pinch and compliant grasp," *IEEE Robotics and Automation Letters*, vol. 5, no. 4, pp. 5518–5525, 2020.

[5] S. Yuan, L. Shao, C. L. Yako, A. Gruebele, and J. K. Salisbury, "Design and control of roller grasper v2 for in-hand manipulation," in *2020 IEEE/RSJ International Conference on Intelligent Robots and Systems (IROS)*, 2020, pp. 9151–9158.

[6] Q. Lu, N. Baron, A. B. Clark, and N. Rojas, "Systematic object-invariant in-hand manipulation via reconfigurable underactuation: Introducing the ruth gripper," *The International Journal of Robotics Research*, vol. 40, no. 12-14, pp. 1402–1418, 2021. [Online]. Available: https://doi.org/10.1177/02783649211048929

[7] L. He, Q. Lu, S.-A. Abad, N. Rojas, and T. Nanayakkara, "Soft fingertips with tactile sensing and active deformation for robust grasping of delicate objects," *IEEE Robotics and Automation Letters*, vol. 5, no. 2, pp. 2714–2721, 2020.

[8] D. Ospina and A. Ramirez-Serrano, "Sensorless In-Hand Manipulation by An Underactuated Robot Hand," *Journal of Mechanisms and Robotics*, vol. 12, pp. 1–26, 03 2020.

[9] T. Chen, M. Tippur, S. Wu, V. Kumar, E. Adelson, and P. Agrawal, "Visual dexterity: In-hand reorientation of novel and complex object shapes," *Science Robotics*, vol. 8, no. 84, p. eadc9244, 2023. [Online]. Available: https://www.science.org/doi/abs/10.1126/scirobotics.adc9244

[10] Y. Tlegenov, K. Telegenov, and A. Shintemirov, "An Open-Source 3D Printed Underactuated Robotic Gripper," 09 2014.

[11] J. Amend and H. Lipson, "The JamHand: Dexterous Manipulation with Minimal Actuation," *Soft Robotics*, vol. 4, no. 1, pp. 70–80, 2017, pMID: 29182098. [Online]. Available: https://doi.org/10.1089/soro.2016.0037

[12] A. Patra and A. J. Spiers, "D-PALI: A Low-Cost Open Source Robotic Gripper Platform for Planar In-Hand-Manipulation," in *2023 IEEE/RSJ International Conference on Intelligent Robots and Systems (IROS)*, 2023, pp. 4540–4546.

[13] A. Spiers, B. Calli, and A. Dollar, "Variable-Friction Finger Surfaces to Enable Within-Hand Manipulation via Gripping and Sliding," *IEEE Robotics and Automation Letters*, vol. PP, pp. 1–1, 07 2018.